

# Structural efficiency of percolation landscapes in flow networks

M. Ángeles Serrano<sup>1</sup> and Paolo De Los Rios<sup>1</sup>

<sup>1</sup>*Institute of Theoretical Physics, LBS, SB, EPFL, 1015 Lausanne, Switzerland*

Complex networks characterized by global transport processes rely on the presence of directed paths from input to output nodes and edges, which organize in characteristic linked components. The analysis of such network-spanning structures in the framework of percolation theory, and in particular the key role of edge interfaces bridging the communication between core and periphery, allow us to shed light on the structural properties of real and theoretical flow networks, and to define criteria and quantities to characterize their efficiency at the interplay between structure and functionality. In particular, it is possible to assess that an optimal flow network should look like a "hairy ball", so to minimize bottleneck effects and the sensitivity to failures. Moreover, the thorough analysis of two real networks, the Internet customer-provider set of relationships at the autonomous system level and the nervous system of the worm *Caenorhabditis elegans*—that have been shaped by very different dynamics and in very different time-scales—, reveals that whereas biological evolution has selected a structure close to the optimal layout, market competition does not necessarily tend toward the most customer efficient architecture.

## I. INTRODUCTION

Despite profound differences, natural and artificial networked systems share striking similarities. Complex networks science [1, 2, 3] has successfully rationalized several of the most ubiquitous features, such as the small world property or the presence of strong degree heterogeneity, relating them to the existence of general organizing principles. These self-organization laws also shape the observed large-scale connectivity layout of a special, yet common, class of networks describing transport processes, be it of matter, energy, or information. These networks are characterized by asymmetric interactions giving rise to local flows that collectively organize into a large-scale stream dominated by a processing core which transfers input into output: the universal bow-tie architecture [4] that is intimately related to the functional activity of these systems.

In general terms, most previous research exploring the relation between form and function in complex networks has been mainly focused on the analysis of topological features such as modular ordering revealing functional aspects [5], with fewer exceptions treating directly functional aspects such as efficiency [6]. Specifically, transport has been studied as one of the main functions influenced by topology [7, 8] and functional design principles of global flux distributions have been discussed for biological networks [9, 10, 11]. Despite these efforts, the "form follows function" assertion still remains to be fully understood from a complex networks science perspective, a major difficulty in the fact that present network patterns are the result of non-stationary and adaptive evolutionary histories that can greatly vary for different networks. However, general self-organization principles should not only govern structure but also their interplay with functional features.

Our purpose of inferring information about function and evolution from a precise knowledge of the topologi-

cal makeup requires the understanding of how flow networks organize to develop functionality. In this respect, percolation theory on complex networks [12] provides a valuable framework to discuss their connectedness and to identify the components that are key to a complete description of their global connectivity layouts conforming the percolation landscapes. This analysis, in turn, allows us to quantify the degree of efficiency that the network has achieved in relation to its operativeness as a global transport system. In particular, the major role played by interfaces, bridging the communication between the different percolation components [13], allowed us to define structural efficiency in terms of two complementary aspects: stress or structural load carried by the interfaces—which also informs about robustness—, and closeness or extent of the direct access to the processing core. We use theoretical arguments to propose the conformation of maximal structural efficiency and demonstrate by the analysis of real networks that biological systems exposed to long-term evolutionary pressure may be much closer to optimality than information technologies systems at an early stage of development dominated by competitive forces.

## II. THE ARCHITECTURE OF PERCOLATION LANDSCAPES

Global communication is essential to develop efficient collective behavior. In flow networks, represented as directed complex networks, global connectivity is ensured by the presence of architectural elements that allow to traverse the network from the input to the output components. These layouts are best rationalized in the framework of percolation theory, so we call them percolation landscapes. Characteristic topologies in the percolated phase denote a global flux that organize in distinct linked components comprising macroscopic portions of the system (Fig. 1 gives a schematic representation). In

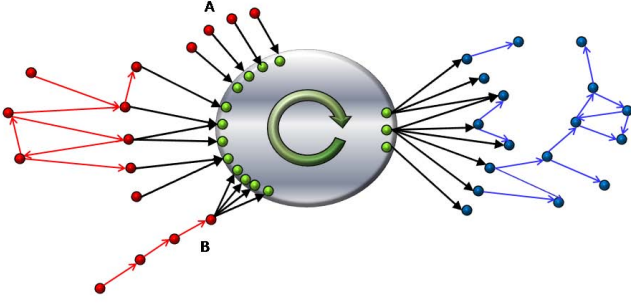


FIG. 1: Schematic diagram of the main components in the percolation landscape of a flow network. The core at the center comprises nodes in the SCC and edges within, forming the SCE. Nodes in red belong to the IN and the ICE is formed by red links. Nodes in blue belong to the OUT and blue links form the OCE. Both interfaces, ITF and OTF, appear in black.

the percolated phase, the traditional node percolation map [14, 15, 16] recognizes a core structure, the giant strongly connected component (SCC), which vertices can communicate with each other following directed paths. In many real systems this core is a processing unit which transfers input to output, and so it is connected to peripheral components. The input comes from an afferent component, the giant in-component (IN), composed by all vertices that can reach the SCC but cannot be reached from it, and the output goes to an efferent component, the giant out-component (OUT), made of all vertices that are reachable from the SCC but cannot reach it. Secondary structures such as tubes or tendrils could also be present [4]. Changing the perspective from nodes to edges, this picture is complemented by the edge percolation map [13], where the number of relevant structures increases to five: the edges pure components, ICE, OCE, and SCE, that are formed by edges connecting nodes within the IN, OUT, and SCC respectively; and edges forming the interfaces, ITF and OTF, that bridge the peripheral components (IN and OUT, respectively) to the core.

This pattern is obviously further shaped by system dependent specificities that are the reflection of functional demands and evolutionary and/or adaptive forces. In particular, the specific conformation of the interfaces determines the structural efficiency and robustness of the network as a global transport system and the potential risk of bottleneck effects.

### A. Percolation landscapes of real networks

We consider here two different information processing systems characterized by global transport phenomena: one socio-technological, the Internet, in contraposition with one biological, the nervous system of the nematode worm *Caenorhabditis elegans* (*C. elegans*). The node and

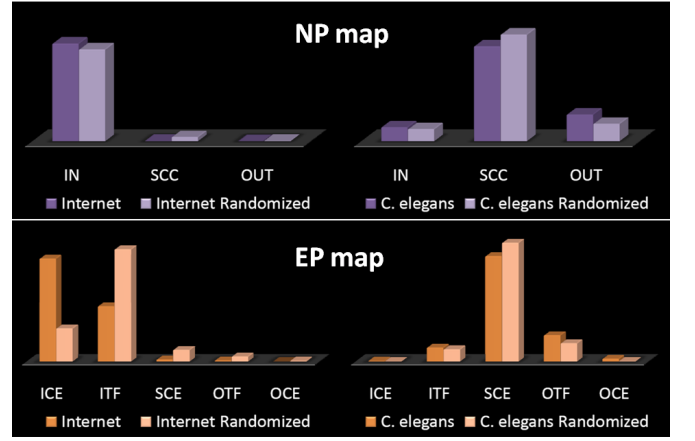


FIG. 2: Bar diagrams of the values showed in Table 1 detailing the percolation landscapes of the ASR and the CEN networks as compared with the randomized counterparts. Top charts in violet show the node percolation maps and bottom charts in orange show the edge percolation maps.

TABLE I: Statistics for the percolation landscapes of the ASR and the CEN networks and their randomized versions (subscript  $R$ , values are average  $\pm$  standard deviation rounded off to the first significative figure). The sizes of the main components are given in absolute number of nodes and links. The average degrees are  $\langle k_i \rangle = \langle k_o \rangle = 1.87$  and  $\langle k_i \rangle = \langle k_o \rangle = 6.82$  respectively. NP stands for Node Percolation map and EP for Edge Percolation map.

		ASR	ASR <sub>R</sub>	CEN	CEN <sub>R</sub>
NP	IN	20060	18900 $\pm$ 800	29	25 $\pm$ 2
	SCC	90	880 $\pm$ 40	195	219 $\pm$ 2
	OUT	17	120 $\pm$ 30	55	36 $\pm$ 2
	Main	20167	19900 $\pm$ 800	279	279 $\pm$ 0
	TOTAL	24545	24545	279	279
EP	ICE	20180	6500 $\pm$ 400	9	3 $\pm$ 2
	ITF	10833	22000 $\pm$ 2000	175	154 $\pm$ 8
	SCE	389	2300 $\pm$ 200	1322	1490 $\pm$ 20
	OTC	226	1000 $\pm$ 100	330	230 $\pm$ 20
	OCE	12	150 $\pm$ 50	36	4 $\pm$ 3
	Main	31640	32000 $\pm$ 2000	1872	1883 $\pm$ 5
	TOTAL	45914	45914	1903	1903

edge percolation maps of their directed network reconstructions are detailed in Fig. 2 and Table 1.

Their maximally random counterparts are also analyzed as null models. In practice, the randomization is achieved at the stationary state of a rewiring process that at each time step randomly selects a couple of links and exchange their ending points [25] avoiding the formation of multiple and self-connections and bidirectional links while preserving the degree distribution  $P(k)$ . The randomized version would preserve as well

degree-degree correlations and higher-order effects which correspond to structural constraints ensuring the realizability of the network [26]. The comparison of real networks with their randomized counterparts makes therefore possible to determine to which extent the measured values are due to global organizing principles and not to random assemblages affected by finite-size effects. In this work, the randomized counterparts are produced out of 10 randomized realizations.

### 1. Internet customer-provider AS relationships (ASR)

The Internet is one of the paradigmatic information technology and communication networks [17]. From an operative point of view, it is composed of thousands of Internet Service Providers, usually identified with autonomous systems (ASs), that operate individual parts of the whole infrastructure and engage in contractual relationships to collectively route traffic through the network. Such business dependencies [18] are mappable to a directed graph representation of unambiguous customer-provider relationships among ASs.

The directed graph is reconstructed from the map 2007-04-02 of inferred AS relationships provided by CAIDA (<http://www.caida.org/data/active/as-relationships/>). Relationships among ASs are usually realized in the form of business agreements, generally simplified to customer-provider, peer-to-peer and sibling-to-sibling. In a purely directed version of the network, where links represent net flow of payments for services provided, relations between siblings immediately cancel out since they administratively belong to the same organization. Peer-to-peer relations are however not trivial because they just freely exchange traffic between themselves and their customers but not up in the hierarchy. Anyway, we assume here that the later are balanced in both directions so as a first approximation we neglect them as well. On the other hand, customer-provider relationships are unambiguously represented by directed edges from customer to provider. We are left with a purely directed network of 24545 nodes and 45914 directed links, after removing 4312 (8.55%) peer-to-peer and 236 (0.47%) sibling-to-sibling relations). The in-degree distribution is very broad and well described by a power law with characteristic exponent 2.1. The out-degree distribution is strongly bounded and decays extremely fast with a maximum out degree of 24.

This network presents an extremely asymmetric structure at the level of the node percolation map, with a huge IN component, a restricted SCC, and an even smaller OUT component (Table 1). By comparison, the randomized counterpart is characterized by a similar IN component, but by ten-fold larger (albeit still small in absolute terms) SCC and OUT components. This information about the node partition should be complemented by the analysis of the edge percolation map to provide a first glimpse of the different architectural organization of

the real versus the randomized network. Again the size in number of edges of the core and the efferent structures (see left graph in Fig. 3 for details about the efferent components) are qualitatively in accordance with the values for the randomized network, despite being smaller. However, the organization of the afferent components is very different from random. The ICE of the real network contains as many edges as nodes in the IN component. Moreover, the number of ITF edges connecting the IN and SCC components is just half the number of IN nodes: on average, thus, there are two IN nodes for every ITF edge, which further implies that many nodes in the in-component lack direct access to the core. By converse, the randomization predicts an ITF double in number of edges than actually observed with a correspondingly reduced ICE, so a more shallow IN.

### 2. Synaptic neuronal structure of *C. elegans* (CEN)

A different family of information transport systems that naturally emerge as archetypical networks are biological nervous systems. As for most other complex networks, their structure is intimately related to their function and the emergent behavior cannot be understood from the mere summation of the individual neuronal actions. We focus on the nervous system of the *C. elegans* worm which is practically completely known [19].

Network representations of brains display neurons as vertices and connection between pairs are present whenever a synapse or gap junction has been observed. We use the updated data set presented in [19] (<http://www.wormatlas.org/>). The pharyngeal system comprises 20 neurons and is almost totally disconnected from the rest of the network. It is excluded along unconnected neurons, as well as connections of the somatic nervous system to non-neural cells. We further restrict to chemical synapses excluding gap junctions, very different from the previous in nature and function. For simplicity, polarity or multiplicity of connections are not taken into account but directionality is. The synapses are directed in nature but 233 reciprocal connections has been detected (12%). We handled this issue by exploiting the imbalance in the number of observed synapses in each direction, so that we preserve the directionality of the larger number. In this treatment, just 58 of them cancel out (3%). The final set contains 279 nodes and 1903 links. As reported previously, it turns out to be a small-world network [23] with tails of the cumulative distribution of degrees for both incoming and outgoing neuronal links that have been reported to be well approximated by exponential decays [24].

Its percolation layout is surprisingly close to random organization. In contrast to the Internet, the main structure consists of a big core with an OUT twice as large as the IN one (see right graph in Fig. 3 for details about the afferent components), in accordance to the randomized counterpart. The number of edges within the peripheral



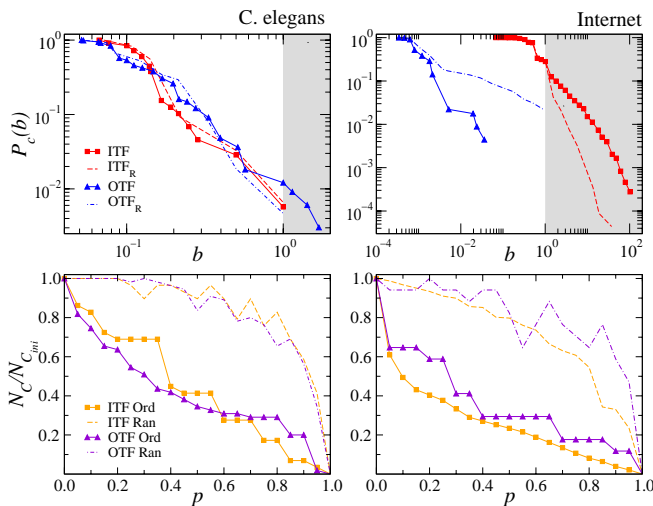


FIG. 4: **Upper row panels.** Cumulative random-walk betweenness distribution for the in- and out-interfaces. The empirical distributions (symbol lines) are compared against those for the randomized null models (dashed lines). **Bottom row panels.** Fraction of nodes remaining in the peripheral components of the real networks after removing a fraction  $p$  of edges of the corresponding interfaces. A targeted removal by load in decreasing order (symbol lines) is compared with a random deletion (dashed lines).

the interface supports. Vector  $b_{jI}/N_P$  corresponds to a normalized probability distribution whenever tendrils or tubes are not considered. The presence of those appendices produce *cul-de-sac* which receive part of the diffusion unloading partially the interfaces.

In Fig. 4 (upper panels), we provide the cumulative distribution  $P_c(b) = \sum_{b' > b} P(b')$  of the values  $b_{jI}$ , the random-walk betweenness for edge  $j$  in interface  $I$  ( $I=ITF$  or  $OTF$ ), which correspond to the loads of the edges at the interfaces of the ASR and CEN networks. The cumulated probability density function of the loads shows that they are not uniformly distributed for either network but have heavy tails denoting large fluctuations, with a few links bearing a much higher level of structural stress. This heterogeneity is not *per se* indicating that the interface is overstressed. The random-walk betweenness is moderately highly correlated with degree [22] meaning that, in general, vertices with higher degree tend also to have higher random-walk betweenness, so that strong disorder in the topology could induce spurious heterogeneity in the load distribution.

In order to assess whether the structural load could represent a potential danger of bottleneck formation in traffic related processes running on the network, one has to define further what is expected as a low load in the situation of maximal structural efficiency. We make the assumption that such efficiency is reached whenever each edge in the interface carries at most a unitary load. This gives a simple criteria which makes possible to compare different networks but also different links of the same

interface. At the same time, the results should be again validated by investigation of the maximally random counterpart. In Fig. 4 (upper panels), grey areas denote stress regions with loads above 1. Whereas the CEN network entirely conforms once more to the randomized prediction with the practical totality of loads below the threshold, most edges of the in-interface of the ASR network appear to be overstressed, a clear indicator of the vulnerability of the system. The region of loads much below 1 usually corresponds to peripheral leaf nodes connected to multiple core nodes. Apart from a signature of local robustness, this diversification could be interpreted as well as a quality of being a peripheral spreader or collector of flow.

Finally, the average stress-related structural efficiency of an interface can be simply approximated as

$$\langle k_B \rangle = \frac{E_I}{N_P}, \quad (1)$$

that is, the average number of interface edges that mediate between peripheral nodes and the SCC. This average coincides with the inverse of the average betweenness of the edges at the interfaces,  $\langle B \rangle_I = \sum_{j \in F} b_{jI}/E_I$ . Higher values of  $\langle k_B \rangle$  are clearly desirable as peripheral nodes would have more routes to the SCC.

## B. Stress and robustness

The loads of the edges at the interfaces are related to their robustness, defined as a measure of the ability of the interfaces to communicate different components under malfunction or failure. In the bottom panels of Fig. 4, we show the fraction of nodes remaining connected in the peripheral components after the removal of an increasing fraction of edges at the corresponding interface. Two different experiments are performed, the first choosing edges according to load in decreasing order and the second selecting them at random. The results prove that although the interfaces seem to be quite robust against random failures, the failure of high load edges would disconnect a bigger portion of peripheral nodes, thus strongly affecting the behavior of the system. The CEN and AS networks substantially differ in this respect. About 40% of interface edges must be removed in CEN before 50% of the peripheral nodes are disconnected from the SCC in the targeted experiment. By converse, the AS network is more delicate because the same degree of disconnection is reached by removing just 20% of the interface edges.

## C. Closeness

The random walk methodology presented above cannot discriminate between peripheral conformations with different access to the SCC if equal loads are associated to interface edges (as a simple example, see tree-like groups  $A$  and  $B$  in Fig.1). The concept of closeness allows us to



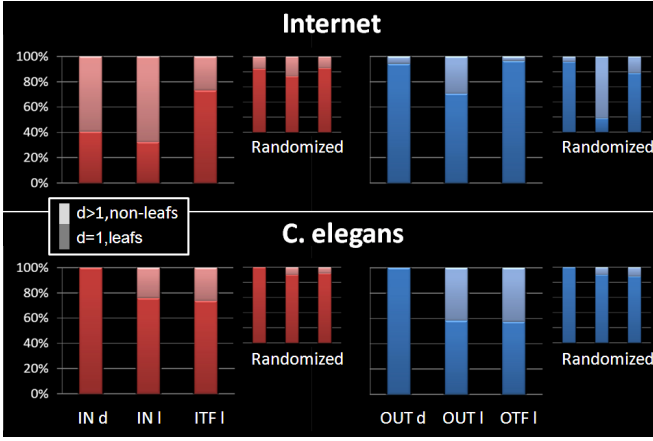


FIG. 5: Bar diagrams summarizing fine details of the peripheral components and the interfaces of ASR and CEN networks as compared with the randomized null models. Charts in red refer to the afferent structure and those in blue to the efferent one. The first two bars in each graph refer to the peripheral node components detailing the proportions of nodes at distance 1 and larger and the proportion of leaf versus non-leaf nodes respectively, and the third bar refers to leaf versus non-leaf edges at the interfaces.

TABLE II: Interfaces and peripheral components fine details for the ASR and CEN networks and their randomized counterparts (subscript  $R$ , average  $\pm$  standard deviation rounded off to the first significative figure). Edges at the interfaces and nodes at the components are separated into leafs ( $l$ ) and non-leafs ( $nl$ ), and nodes directly connected to the core ( $d = 1$ ) are distinguished from those at larger distances ( $d > 1$ ).

	Internet	Internet <sub>R</sub>	C. elegans	C. elegans <sub>R</sub>
IN <sub>d=1</sub>	40.71%	84% $\pm$ 1%	100.00%	100% $\pm$ 0%
IN <sub>d&gt;1</sub>	59.29%	16% $\pm$ 1%	00.00%	0% $\pm$ 0%
IN <sub>l</sub>	32.34%	74% $\pm$ 1%	75.86%	90% $\pm$ 6%
IN <sub>nl</sub>	67.66%	26% $\pm$ 1%	24.14%	10% $\pm$ 6%
ITF <sub>l</sub>	73.23%	84.8% $\pm$ 0.2%	73.71%	92% $\pm$ 5%
ITF <sub>nl</sub>	26.77%	15.2% $\pm$ 0.2%	26.29%	8% $\pm$ 5%
OUT <sub>d=1</sub>	94.12%	93% $\pm$ 4%	100.00%	100% $\pm$ 0%
OUT <sub>d&gt;1</sub>	5.88%	7% $\pm$ 4%	0.00%	0% $\pm$ 0%
OUT <sub>l</sub>	70.59%	18% $\pm$ 3%	58.18%	90% $\pm$ 6%
OUT <sub>nl</sub>	29.41%	80% $\pm$ 3%	41.82%	10% $\pm$ 6%
OTF <sub>l</sub>	96.46%	78% $\pm$ 9%	57.27%	88% $\pm$ 7%
OTF <sub>nl</sub>	3.54%	22% $\pm$ 9%	42.73%	12% $\pm$ 7%

shed light on the different efficiencies that characterize these dissimilar architectures.

By convention, leaf vertices are those with in-degree 0 or out-degree 0, so that they are restricted to belong to a peripheral component. In-leaf edges (out-leaf edges) are considered as directed links leaving from (pointing to) a leaf vertex[27]. Non-leaf edges in the interfaces are the

TABLE III: Structural efficiency average degrees for ASR and CEN and their randomized counterparts (subscript  $R$ , values are average  $\pm$  standard deviation rounded off to the first significative figure). Infinite closeness averages come from the fact of all peripheral nodes being directly connected to the core.

	ASR	ASR <sub>R</sub>	CEN	CEN <sub>R</sub>
$\langle k_B \rangle_{IN}$	0.54	1.15 $\pm$ 0.04	6.03	6.3 $\pm$ 0.3
$\langle k_C \rangle_{IN}$	0.24	1.1 $\pm$ 0.1	$\infty$	$\infty \pm 0$
$\langle k_B \rangle_{OUT}$	13.29	8 $\pm$ 1	6.00	6.5 $\pm$ 0.2
$\langle k_C \rangle_{OUT}$	8.00	30 $\pm$ 20	$\infty$	$\infty \pm 0$

ones that ensure the communication from/to nodes not directly connected to the core. These non-leaf edges are the potentially responsible for bottleneck effects, since they service from more than a single IN or OUT node. A first estimate of how this topological considerations affects efficiency at the structural level is given by the closeness average degree,

$$\langle k_C \rangle = \frac{E_{I,nl}}{N_{P,d>1}}, \quad (2)$$

which is the number of interface non-leaf edges available for each peripheral node which is not directly connected to the SCC (thus, with a distance  $d$  from the SCC greater than 1).

Values for the decomposition of the ASR and CEN interfaces and the peripheral components into leafs and non-leaf units along with average degree efficiency measures as defined in Eq. (1) and Eq. (2) are shown in Table 2, Table 3, and Fig. 5. In general terms, the higher the averages the more structurally efficient the system is expected to be. An important imbalance is observed between the in and out values for ASR. According to the average values, the in-interface presents a certain level of inefficiency, with low average degrees combined with a low number of leafs, much below random expectations. In this situation, potential bottleneck effects are more likely. In contrast, the out component shows high levels of structural efficiency, with the practical totality of nodes being root nodes directly connected to the core. On the other hand, all peripheral CEN nodes have direct access to the core, a signature of high efficiency.

#### D. Maximum structural efficiency and the “hairy” ball

Under the requirements of low stress and high closeness, and in the approximation of inexpensive edges, maximum efficiency would be realized by a percolation landscape structured as a perfect “hairy ball”, with all the nodes in the peripheral components directly attached to the core through leaf edges, each carrying at most a

unitary load [28], thus without endangering bottleneck effects. Moreover, the interfaces would be robust because the failure or malfunctioning of any of its edges would affect a minimum number of nodes in the peripheral components. Finally, all peripheral nodes would have direct access to the core. Any departure from the “hairy ball” paradigm would lead to situations in which at least one of the two or both requests for structural efficiency, low stress and high closeness, are violated to some degree.

#### IV. CONCLUSIONS

Our thorough analysis of percolation landscapes shows that the conformation of interfaces plays a central role in the performance of complex flow networks as global transport systems, governing their efficiency against bottlenecks and their robustness against failures. We highlight that, from the purely structural efficiency perspective, a “hairy ball” design would be optimal. Appealingly, such behavior may be even displayed by a very close to random architecture as seen for the synaptic neuronal network of *C. elegans*. Of the two real systems analyzed in this work, this is the one much closer to such optimality whereas the Internet network presents inefficiencies. These findings point to two, not mutually exclusive, interpretations. On the one hand, different adaptation dynamics are surely at work: whereas the present structure of the *C. elegans* nervous system tries to optimize its *collective* performance without inter-neuron competition, the Internet network emerges, due to its customer-provider relations, as a competitive network where it is

not the global optimization which is sought for but rather the individual Internet service provider gain. In this respect, global efficiency is important only in relation to its marketable value. Interestingly, the Internet customer-provider network outperforms its randomized version in the OTF and OUT components, which describe the ultimate cash flow, and underperforms it in the afferent components, where end-users are. On the other hand, evolution of the worm nervous system might have allowed better architectures to emerge, due to its evolutionary time-scale (hundred of millions of years) running much longer than the time-span of existence of the commercial Internet network (slightly more than ten years).

Clearly, these results only shed light on the basic structural ingredients for efficiency and robustness. Indeed, several other constraints (*e.g.* costs of edge deployment and maintenance or capacity), are at play which should be taken into account for more precise and system specific analysis. Yet, percolation landscapes represent a first general framework to highlight potential problems in a network structure, possibly suggesting specific actions to reinforce stressed elements or the redistribution of loads so to reduce the risk of bottlenecks and the impacts of failures.

#### Acknowledgments

The authors thank Marián Boguñá for useful comments and discussions. This work has been financially supported by DELIS under contract FET Open 001907 and the SER-Bern under contract 02.0234.

- 
- [1] R. Albert and A.-L. Barabási, *Rev. Mod. Phys.* **74**, 47 (2002).
  - [2] S. N. Dorogovtsev and J. F. F. Mendes, *Evolution of networks: From biological nets to the Internet and WWW* (Oxford University Press, Oxford, 2003).
  - [3] M. E. J. Newman, *SIAM Review* **45**, 167 (2003).
  - [4] A. Broder, R. Kumar, F. Maghoul, P. Raghavan, S. Rajagopalan, S. Stata, A. Tomkins, and J. Wiener, *Computer Networks* **33**, 309 (2000).
  - [5] R. Guimerà, M. Sales-Pardo, and L. A. N. Amaral, *Nature Physics* **3**, 63 (2007).
  - [6] V. Latora and M. Marchiori, *Phys. Rev. Lett.* **87**, 198701 (2001).
  - [7] E. L. Z. T. S. Sreenivasan, R. Cohen and H. E. Stanley, *Physical Review E* **75**, 036105 (2007).
  - [8] L. K. Gallos, C. Song, S. Havlin, and H. A. Makse, *Proc. Natl. Acad. Sci. USA* **104**, 77467751 (2007).
  - [9] E. Fischer and U. Sauer, *Nature Genetics* **37**, 636 (2005).
  - [10] M. Csete and J. Doyle, *TRENDS in Biotechnology* **22**, 446 (2004).
  - [11] D. Segrè, D. Vitkup, and G. M. Church, *Proc. Natl. Acad. Sci. USA* **99**, 15112 (2002).
  - [12] M. E. J. Newman, S. H. Strogatz, and D. J. Watts, *Phys. Rev. E* **64**, 026118 (2001).
  - [13] M. A. Serrano and P. D. L. Rios, arXiv:0706.3156v1 [cond-mat.dis-nn] (2007).
  - [14] M. Boguñá and M. A. Serrano, *Phys. Rev. E* **72**, 016106 (2005).
  - [15] S. N. Dorogovtsev, J. F. F. Mendes, and A. N. Samukhin, *Phys. Rev. E* **64**, 066110 (2001).
  - [16] M. E. J. Newman, *Phys. Rev. Lett.* **89**, 208701 (2002).
  - [17] R. Pastor-Satorras and A. Vespignani, *Evolution and Structure of the Internet. A Statistical Physics Approach* (Cambridge University Press, Cambridge, 2004).
  - [18] X. Dimitropoulos, D. Krioukov, M. Fomenkov, B. Hufaker, Y. Hyun, K. Claffy, and G. Riley, *ACM SIGCOMM Computer Communication Review* **37**, 29 (2007).
  - [19] B. L. Chen, D. H. Hall, and D. B. Chklovskii, *Proc. Natl. Acad. Sci. USA* **103**, 4723 (2006).
  - [20] S. Achard and E. Bullmore, *PLOS Computational Biology* **3**, 174 (2007).
  - [21] L. Freeman, *Sociometry* **40**, 3541 (1977).
  - [22] M. E. J. Newman, *Social Networks* **27**, 39 (2005).
  - [23] D. J. Watts and S. H. Strogatz, *Nature* **393**, 440 (1998).
  - [24] L. A. N. Amaral, A. Scala, M. Barthélemy, and H. E. Stanley, *Proc. Natl. Acad. Sci. USA* **97**, 11149 (2000).
  - [25] S. Maslov and K. Sneppen, *Science* **296**, 910913 (2002).
  - [26] M. Boguñá, R. Pastor-Satorras, and A. Vespignani, *Eu-*

ropean Physical Journal B **38**, 205 (2004).

- [27] Strictly speaking, vertices with in-degree 0 are usually referred as root vertices. We refer to them as leaf vertices for economy of language. Note also that according to the definitions of in-leaf (out-leaf) edges, the in (out) interface cannot contain out-leaf (in-leaf) edges and that from the perspective of vertices the definitions would be

reversed.

- [28] The absence of nodes at distances larger than 1 could involve a marginal deviation from the “hairy ball” conformation with a few loads slightly greater than 1 due to inner connections in the peripheral component.